⌘ *Author's Choice*

THE JOURNAL OF BIOLOGICAL CHEMISTRY VOL. 286, NO. 23, pp. 20152–20162, June 10, 2011

A Zinc Finger Protein, TbZC3H20, Stabilizes Two Developmentally Regulated mRNAs in Trypanosomes*[S]

Received for publication, April 29, 2010, and in revised form, April 1, 2011 Published, JBC Papers in Press, April 5, 2011, DOI 10.1074/jbc.M110.139261

Alexandra S. Ling, James R. Trotter, and Edward F. Hendriks[1]

From the Division of Cell and Molecular Biology, Imperial College London, South Kensington Campus, London SW7 2AZ, United Kingdom

CCCH zinc finger proteins (ZC3Hs) are a novel class of RNA-binding protein involved in post-transcriptional mechanisms controlling gene expression. We show TbZC3H20 from *Trypanosoma brucei*, the causative agent of sleeping sickness and other diseases, stabilizes two developmentally regulated transcripts encoding a mitochondrial carrier protein (MCP12) and *trans*-sialidase (TS-like E). TbZC3H20 is shown to be an RNA-binding protein that is enriched in insect procyclic form *T. brucei* and is the first ZC3H discovered controlling gene expression through modulating mRNA abundance in trypanosomes. Previous studies have demonstrated that RNA recognition motif-containing and PUF family RNA-binding proteins can control gene expression by stabilizing specific target mRNA levels. This work is the first to describe a ZC3H stabilizing rather than destabilizing target mRNAs as a regulatory mechanism and the first report of a ZC3H regulating a gene encoding a mitochondrial protein. This suggests a broader role for ZC3Hs in post-transcriptional regulation of gene expression than previously thought.

Transcriptional control is central in governing many cellular processes. However, post-transcriptional regulation, including mRNA processing, localization, turnover, and translation, add to the complexity and flexibility of gene expression (1). Post-transcriptional control mechanisms of gene expression are dependent on RNA-binding proteins (RBPs),[2] which are ubiquitous and numerous in most eukaryotic genomes (2). One fundamental aspect of post-transcriptional control of gene expression is, therefore, to define which RNA in a cell is regulated by a particular RBP and the mechanism by which regulation is achieved. The interaction of target RNA and RBP is often reliant on sequence elements in the 3′-untranslated region (3′-UTR) of the target transcript, and this governs the mechanism of regulation of gene expression either via transcript stability or translational efficiency (3). In many organisms the basic associations of mRNAs and RBP are poorly defined and the control mechanism unknown, leaving a significant gap in understanding regulated gene expression.

Kinetoplastids, such as *Trypanosoma brucei*, *Trypanosoma cruzi*, and *Leishmania major* are protozoan parasites responsible for sleeping sickness, Chagas disease, and leishmaniasis in humans. The kinetoplastids diverged very early in the eukaryotic lineage (4, 5), and interestingly, kinetoplastids arrange their genes into long polycistrons (10s-100s of units in length), and their genomes encode few potential transcription factors (6). These polycistronic units have genes co-transcribed and subsequently processed by coupled 5′ trans-splicing and 3′ polyadenylation before translation (7). Thus, trypanosomes seem to have lost the ability to regulate the initiation of RNA polymerase II-dependent transcription, and trypanosome gene expression is regulated primarily at the post-transcriptional level (8). Processing of mRNA and transport are important parts of the gene expression machinery, which appear largely conserved among eukaryotes but do not seem to represent a major regulatory point in trypanosomes. Published works suggest the main point for controlling gene expression in trypanosomes is at the level of mRNA turnover and translational efficiency (9).

Trypanosomes have life cycles in both a mammalian host and an invertebrate vector. Adaptation to these very different environments requires significant alteration in gene expression (10, 11). Consequently, surface protein expression, metabolism changes, and the cytoskeletal alterations that accompany parasite development during the life cycle must all involve post-transcriptional control of gene expression. The major replicative stages of *T. brucei* are the mammalian bloodstream form (BF) and insect procyclic form (PF). Several studies have been conducted indicating developmental regulation of ~200–300 transcripts in each life cycle stage (12–14), and the differential abundance of specifically enriched BF or PF transcripts are assumed to be governed via mRNA stability (13). To date very little is known about the RBPs that are involved in regulating target mRNA abundance of developmentally regulated transcripts.

Zinc finger proteins are a large superfamily, and they constitute about 1% of many eukaryotic genomes (15). Zinc finger proteins are categorized according to the nature and spacing of their zinc-chelating residues. Several families of zinc finger proteins, including the C2H2s, CCHCs, and CCCCs, have important functions as transcription factors that regulate a range of biological processes (16). Most zinc finger protein families are, therefore, associated with DNA binding or protein-protein interactions (15). However, several investigations have shown CCCH zinc finger proteins (ZC3Hs) to be involved in RNA binding (17). ZC3Hs are rare in number in many lower eukaryotes and in mammals (18) but have been found in a vari-

* This work was funded by the Wellcome Trust.

[S] The on-line version of this article (available at http://www.jbc.org) contains supplemental Table 1, Figs. 1 and 2, and Arrays 1, 2, and 3.

⌘ *Author's Choice*—Final version full access.

[1] To whom correspondence should be addressed. Tel.: 44-020-759-43091; Fax: 44-020-759-43095; E-mail: e.hendriks@imperial.ac.uk.

[2] The abbreviations used are: RBP, RNA-binding protein; BF, bloodstream form; PF, procyclic form; ARE, AU-rich element; TAP, tandem affinity purification; MCP, mitochondrial carrier protein; qPCR, quantitative PCR.

ety of organisms ranging from yeast to man (19). RBPs have been shown to regulate mRNA abundance through a number of sequences, most notably AU-rich elements (AREs) found in the 3′-UTR of target transcripts (3, 20). Most studies on ZC3Hs have been conducted using the tandem ZC3H protein, tristetraprolin, and ARE-containing transcripts important in immune responses, like TNF-α (21), have been identified as targets. In all cases where mRNA abundance of a target transcript is altered by a ZC3H, the mechanism of regulation involves destabilization. Some proteins containing variant ZC3H motifs, such as ZAP, have anti-viral properties (22). Several ZC3Hs from *Caenorhabditis elegans* have also been shown to be involved in the regulation of development through RNA localization in the cell (23). There have been studies on three ZC3Hs in trypanosomes (TbZFP1, -2, and -3) (24–26). Only TbZFP3 has been investigated for a regulatory mechanism and found to control the expression of the variant forms of the insect stage-specific surface protein coat via translational repression rather than transcript stability (27). Thus, the ZC3Hs represent a novel and exciting family of RBPs involved in post-transcriptional control of gene expression.

This study investigates one member of the *T. brucei* ZC3Hs, TbZC3H20. TbZC3H20 is shown to bind RNA *in vitro* and *in vivo* and is stage-specifically enriched in PF when compared with BF parasites. TbZC3H20 was also found to be required for normal growth of PF parasites. Using a combination of microarray analyses and RNAi, TbZC3H20 was found to control the mRNA abundance of two developmentally regulated transcripts encoding a mitochondrial carrier protein (MCP12) and a *trans*-sialidase (TS-like E). Here we demonstrate TbZC3H20 is involved in specific stabilization of these mRNAs in PF *T. brucei* via elements in the 3′-UTR of each transcript. The specific target mRNAs of TbZC3H20 defined in this study are important in the development of *T. brucei*, and understanding their regulation is a key part in understanding the life cycle of trypanosomes. This study is the first report of a ZC3H regulating a gene encoding a mitochondrial protein and the first to show ZC3Hs can regulate mRNA abundance (stability) as a post-transcriptional mechanism for regulating gene expression in trypanosomes. Most significantly, this work shows ZC3H-dependent stabilization rather than destabilization of a target mRNA, suggesting a broader involvement of ZC3Hs in regulating gene expression than previously thought.

EXPERIMENTAL PROCEDURES

Plasmid Constructs—Oligonucleotides used in this study are shown in supplemental Table 1. The entire coding region of TbZC3H20 was PCR-amplified from *T. brucei* genomic DNA (strain 427) using primers that incorporated restriction enzyme sites HindIII and BglII or BglII and EcoRI. The PCR products were cloned first into the pGEM-T Easy Vector (Promega) (to create pGEM 20) as described by the manufacturer and then into p2T7i (28) (creating p2T7i 20) for tetracycline (tet)-inducible double-stranded RNA production (RNAi) or the *Escherichia coli* expression vector pGEX-2T. The pGEM 20 construct was also used to introduce a point mutation from CCCH to CCAH for each zinc finger motif of TbZC3H20. The first CCCH zinc finger motif was mutated (C70A) using the QuikChange® II site-directed mutagenesis kit (Stratagene) with the TbZC3H20 CCCH ZFM1 F and TbZC3H20 CCCH ZFM1 R primers (supplemental Table 1) by the manufacturer's recommended protocol. The single site-directed mutant was verified by sequencing and then used in a subsequent round of mutagenesis using the same kit and protocol but with the TbZC3H20 CCCH ZFM2 F and TbZC3H20 CCCH ZFM2 R primers (supplemental Table 1) to introduce the mutation into the second zinc finger motif (C178A). This double site-directed mutant was verified by sequencing and then subcloned into the pGEX2T vector. The pLEW79-TbZC3H20-TAP construct was created as in Panigrahi *et al.* (29), except the coding sequence used was that of TbZC3H20. For luciferase reporter assay constructs, the 3′-UTR of MCP12 and TS-like E were PCR-amplified from *T. brucei* genomic DNA using primers incorporating BamHI and XhoI restriction enzyme sites. PCR products were cloned into pGEM T-easy then subcloned into pGR86 (30).

Heterologous Expression in E. coli, Homopolymer RNA Binding Assays, Antibody Production, and Western Analysis—BL21 *E. coli* transformants, cultured in LB plus 100 μg/ml ampicillin at 37 °C, and grown to A_{600} 0.4–0.6 were induced with 0.1 mM isopropyl 1-thio-β-D-galactopyranoside and left at 17 °C overnight shaking. After induction the cells were pelleted and resuspended in BugBuster (Novagen). The lysate was filtered through a 0.45 μm filter then applied to a GSTrapFF column (GE Healthcare) previously equilibrated with PBS. The column was then washed with 5 volumes of PBS, and proteins were eluted with 50 mM Tris-HCl and 10 mM reduced glutathione, pH 8.0. The concentration of eluted protein was quantified by Bradford Assay. To 50 μl of "poly(A)/C/T/G"-Sepharose /agarose beads (Sigma), 500 nmol of GST-purified recombinant TbZC3H20 was added with 20× binding buffer (10 mM Tris-HCl, pH 7.4, and 50 mM sodium chloride final concentrations) and then rotated for 1 h at 4 °C. The beads were then washed 4 times in 1 ml of wash buffer (100 mM sodium chloride) with incubations for 10 min at 4 °C. Finally, beads were resuspended in 4× Laemmli buffer and analyzed by SDS-PAGE.

For Western analysis, proteins were transferred from SDS-PAGE to nitrocellulose by electroblotting. The membrane was blocked in 5% milk with PBS overnight at 4 °C, washed in PBS, and then incubation in the anti-peptide TbZC3H20 antibody for >3 h at 4 °C. The membrane was then washed 3 times in PBS, then incubated with swine anti-rabbit antibody conjugated to HRP (DakoCytomation) at 1:2000 dilution in PBS-Tween (0.1%) for 1 h at 4 °C. The chemiluminescence signal was detected using Pierce® ECL West Femto Western blotting substrate (Thermo Scientific) and captured using a LAS-3000 Fuji imager. Anti-peptide antibodies were produced in rabbits to the TbZC3H20 C-terminal peptide CGTDRGIEKGEGRGRN by Eurogentec. Crude serum was affinity-purified against the peptide (Eurogentec), and this used (1:10) in 1% BSA/PBS for Western analysis.

Trypanosomes—*T. brucei* PF 29-13 cells and PF WT were cultured in SDM-79 medium containing 15% FBS at 27 °C. PF 29-13 cells had been previously engineered to co-express T7 RNA polymerase and tet repressor (31) and were used to generate PF RNAi lines (29-13 cells). PF transfections were carried out as described in Hendriks *et al.* (32). Stable transfectants

were induced for RNAi with 1 μg/ml tet, and the uninduced and induced cells were counted daily with a Z1 Coulter Counter (Beckman Coulter). Cells were maintained between 2×10^6 and 2×10^7 cells/ml. Genomic DNA was extracted from stable transfectants as described in Rotureau *et al.* (55).

RNA Isolation and Northern Analysis; Transcriptional and Translational Inhibition—Trypanosome RNA was prepared from $1–2 \times 10^8$ cells from BF and PF cells, grown in the presence or absence of tet and/or inhibitors (cycloheximide/actinomycin D) when required using the RNeasy kit as described by the manufacturer (Qiagen). RNA concentration was determined using a Nanodrop ND-1000. For Northern analysis 3 μg of RNA was electrophoresed on formaldehyde agarose gels and transferred to nylon membrane by capillary blotting. Blots were hybridized at 65 °C with riboprobes labeled with digoxigenin (Roche Applied Science), and stringency washes were at 65 °C, 0.1× SSC. Blot detection was by chemiluminescence using CDP-star (Roche Applied Science) as a reaction substrate. To quantify the level of transcript in each sample, densitometry of the signal obtained on a FujiFilm LAS-3000 was performed using QuantityONE software. Loading was equalized by the concentration of RNA loaded and signal obtained with tubulin or actin. Measurements for the rate of mRNA turnover in PF *T. brucei* were performed after treatment of cells with 5 $\mu g' ml^{-1}$ actinomycin D for 1, 2, or 4 h. Translational inhibition studies were conducted on samples treated with 50 $\mu g' ml^{-1}$ cycloheximide for 1, 2, or 4 h. Untreated samples for both the actinomycin D and cycloheximide transcription and translation analyses were also prepared from PF *T. brucei*.

Reverse Transcriptase PCR (RT-PCR) and Quantitative Real-time PCR (qPCR)—Primer sequences for qPCR are in supplemental Table 1. qPCR was performed as described previously (33) using the ABI Prism 7700 Sequence Detection System (Applied Biosystems). In both RT-PCR and qPCR experiments, RNA was treated with DNase I by using the DNase-free kit (Ambion). Integrity of the DNase I treated RNA was confirmed by using an RNA nanochip on a BioAnalyzer (Agilent Technologies). Amplification conditions for qPCR were 50 °C for 2 min and 95 °C for 10 min followed by 40 cycles of 95 °C for 15 s and 60 °C for 1 min. Each mRNA species was analyzed in triplicate. Thermal dissociation and agarose gel electrophoresis confirmed PCR generated a single product of the expected size. Data analysis was carried out by using the Pfaffl method with PCR efficiencies calculated by linear regression with LinRegPCR software (34, 35). Relative changes for target amplicons were calculated after normalization to β-tubulin mRNA and 18 S rRNA and were expressed as relative mRNA abundance from the respective control cells. To amplify interacting mRNA species with tandem affinity purification (TAP)-tagged TbZC3H20, RT-PCR was used with gene specific oligonucleotides within the coding regions (supplemental Table 1). RT-PCR reactions were performed in a standard thermocycler using TaqDNA polymerase. Amplification conditions were 95 °C for 5 min followed by 40 cycles of 95 °C for 30 s and 50 °C for 90 s and 90 s at 72 °C. Amplification products were analyzed by agarose gel electrophoresis.

Microarray Analysis—For the microarray samples, PF29-13 p2T7i TbZC3H20 were grown in the presence or absence of tet for 48 h, and then RNA was isolated from $1–2 \times 10^8$ cells using the RNeasy kit as described by the manufacturer (Qiagen). RNA concentration was determined using an ND-1000 NanoDrop spectrophotometer. RNA samples were sent to Oxford Gene Technology Limited for microarray analysis. Three 60-mer gene-specific probes were synthesized for each gene across the *T. brucei* genome, where each probe was synthesized *in situ* directly onto each microarray chip. The RNA samples were labeled with Cy3 (green) or Cy5 (red), and each microarray set was carried out in triplicate, with a dye-switch for one of the replicates. Raw data were transformed into Excel spreadsheets (Microsoft Office) for green and red signal comparison (with background signal subtracted) to determine -fold change for each microarray probe.

Purifying TAP-tagged TbZC3H20 mRNA Complexes—Expression of TbZC3H20-TAP in PF cells was induced for 48 h with tet, and TAP-tagged complexes were purified from 2 liters of cells harvested at a density of 1.5×10^7 cells ml^{-1}. Cells were harvested by centrifugation at 4 °C at 1300 × *g* for 10 min, washed in cold PBS with 6 mM glucose, and resuspended in 18 ml of cold IPP150 (10 mM Tris-HCl, pH 8.0, 150 mM NaCl, 0.1% Igepal) and 2 ml of 10% Triton-X100. Cells were lysed by rotation at 4 °C for 25 min and then centrifuged at 4 °C at 10,000 × *g* for 15 min to remove insoluble material. 200 μl of IgG Sepharose beads ("fast-flow," GE Healthcare) were washed in IPP150 in an Econo-Pac column (Bio-Rad) at 4 °C for 5 min, then the cleared cell lysate was added to the washed column and rotated for 2 h at 4 °C to allow binding. The column was washed 3 times in 10 ml of cold IPP150 and once with 10 ml of cold tobacco etch virus cleavage buffer (10 mM Tris-HCl, pH 8.0, 150 mM NaCl, 0.1% Igepal, 0.5 mM EDTA, 1 mM DTT). The TAP tag was then cleaved by adding 1 ml of tobacco etch virus cleavage buffer and 100 units of tobacco etch virus protease (Invitrogen) and incubated the beads for 2 h at 16 °C. To the tobacco etch virus eluate recovered from the column, 3 volumes of CBB (10 mM Tris-HCl, pH 8.0, 150 mM NaCl, 0.1% Igepal, 10 mM β-mercaptoethanol, 1 mM magnesium acetate, 1 mM imidazole, 2 mM calcium chloride) and 3 μl of 1 M calcium chloride per ml of eluate was added. 200 μl of calmodulin resin was added to a disposable 5-ml column and washed for 5 min at 4 °C with 5 ml of CBB. The sample was then transferred to the column containing the washed calmodulin resin and rotated for 1 h at 4 °C. The column was washed 5 times with 5 ml of CBB, and then the TbZC3H20-mRNA complexes were eluted with 250 μl of CEB (10 mM Tris-HCl, pH 8.0, 150 mM NaCl, 0.1% Igepal, 10 mM β-mercaptoethanol, 1 mM magnesium acetate, 1 mM imidazole, 2 mM EGTA). To this recovered eluate, 0.5 ml of TRI Reagent® (Sigma) was added and incubated at room temperature for 5 min. Isolation of RNA was then carried out as per the manufacturer's instructions, and the RNA pellet was resuspended in 10 μl of RNase-free water. The entire sample was then DNase-treated and reverse-transcribed as described above.

RNA Electrophoretic Mobility Shift Assay (EMSA)—In vitro transcribed RNAs were prepared using DNA templates and either SP6 or T7 RNA polymerase with NTPs at 37 °C for 2 h. RNA EMSA reaction mixtures (10 μl) contained 5 ng of digoxigenin-labeled (UTP) RNA and GST-TbZC3H20, GST TbZC3H20 ZFM mutant, or GST protein (500 nM) as indicated

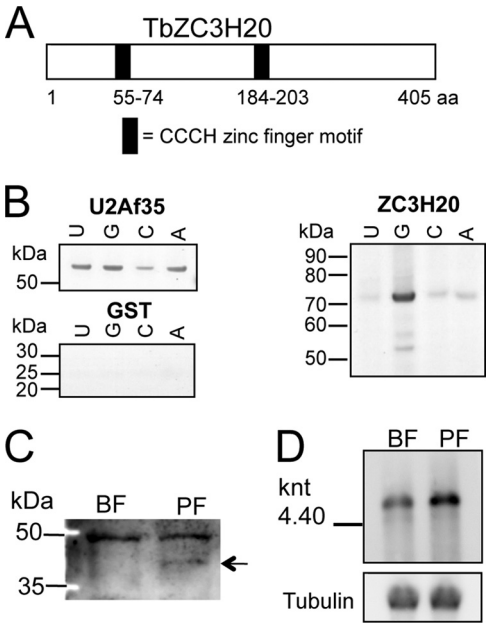

FIGURE 1. **TbZC3H20 is a PF-enriched RBP.** *A*, shown is a schematic representation of TbZC3H20 illustrating the position (in amino acids (*aa*)) of the CCCH zinc finger domains within the protein. *B*, shown is Coomassie Blue-stained SDS-PAGE of purified recombinant GST, GST-TbU2Af35, and GST-TbZC3H20 binding RNA homopolymers (U, G, C, and A) linked to Sepharose beads. Protein markers indicate the size of the recombinant proteins, in line with the expected sizes (GST = 26 kDa, GST-TbU2Af35 = 60 kDa, and GST-TbZC3H20 = 70kDa). *C*, shown is a Western analysis of BF and PF *T. brucei* using the anti-peptide antibody against TbZC3H20. A band of 50 kDa present in both BF and PF is a nonspecific protein that conveniently acts as a loading control. The TbZC3H20 band at 43 kDa is below the level of detection in BF but is detectable in the PF protein sample (position indicated by *arrow*). *D*, a Northern blot shows the size and relative expression level of the TbZC3H20 transcript in BF and PF *T. brucei*. The same RNA samples were hybridized with tubulin to indicate loading. *knt*, kilonucleotides.

in a binding buffer of 50 mM Tris, pH 7.0, 150 mM NaCl, 0.25 mg/ml tRNA, and 0.25 mg/ml BSA. Competition assay reactions contained 500 nM GST-TbZC3H20 and 5 ng of labeled RNA with increasing amounts (ratios 1:0–1:200) of unlabeled competitor RNA. Each reaction was incubated at 37 °C for 10 min with gentle agitation and then prepared for loading with the addition of 1 μl of Bluejuice™ Gel Loading buffer (Invitrogen). The entire mixture was loaded onto a 0.8% agarose gel in TAE buffer and electrophoresed at 25–40 V for 3–6 h. The RNA was then transferred to a nylon membrane by capillary blotting. Blot detection was by chemiluminescence using CDP-star as a reaction substrate, and images were captured by a Fujifilm LAS-3000.

Computing—GeneDB (36) was used for Trypanosome genome sequence data information.

RESULTS

TbZC3H20 Binds RNA and Is Enriched in PF Parasites—Searching the *T. brucei* genome dataset for CCCH zinc fingers (TbZC3Hs) identified 49 proteins bearing the $CX_{7-8}CX_5CX_3H$ motif (6). Only one ZC3H, TbZC3H20, was *T. brucei*-specific with solely conventional ZC3H motifs (37). Thus, as part of analyzing the family of TbZC3Hs, an investigation on TbZC3H20, a ZC3H containing two $C_7C_5C_3H$ motifs (Fig. 1*A*), was performed. To assess if TbZC3H20 could bind RNA, recombinant TbZC3H20 protein fused to glutathione *S*-transferase (GST) was produced in *E. coli* and used in an RNA homopolymer binding assay. Heterologous expression of GST-TbU2Af35, a known RBP, and GST-alone were performed as positive and negative controls. Proteins were purified using GST affinity chromatography, and proteins of the expected size (70 kDa for TbZC3H20, 60 kDa for U2AF35, and 26 kDa for GST-alone) were confirmed by SDS-PAGE (not shown). Each protein (500 nmol) was individually allowed to bind polyU or-G or -C or -A linked to Sepharose beads. Protein binding RNA was revealed on SDS-PAGE stained with Coomassie Blue (Fig. 1*B*), showing GST-TbZC3H20-bound homopolymeric RNA, perhaps with a preference for polyG. The GST-TbU2Af35-positive control protein bound RNA as expected, whereas a negative control of GST protein alone did not bind homopolymeric RNA (Fig. 1*B*). Thus, recombinant TbZC3H20 is capable of binding RNA *in vitro*. To determine the level of TbZC3H20 protein in *T. brucei*, attempts were made to raise antibodies to the recombinant GST-TbZC3H20 in both mouse and rabbit, but this proved unsuccessful. Therefore, a TbZC3H20 anti-peptide antibody immunization was performed, and antibodies were raised in rabbit. Western blot analysis of proteins from BF and PF parasites, using the TbZC3H20 anti-peptide anti-serum, revealed a protein of the correct predicted molecular mass (44 kDa) in PF cells (*arrow* in Fig. 1*C*) but was below the level of detection in BF cells. Western analysis with this TbZC3H20 antibody also showed a nonspecific reacting protein of ~50 kDa (Fig. 1*C*), which was also present in pre-immune serum (see supplemental Fig. 1) and acts as a loading control. Northern analysis of BF and PF RNA showed the presence of a large (>5 kilonucleotides) mRNA for TbZC3H20 in both BF and PF life cycle stages (Fig. 1*D*). Collectively, these results indicate that TbZC3H20 is an RBP that is enriched in PF *T. brucei*.

TbZC3H20 Is Required for Growth in PF T. brucei—To assess whether TbZC3H20 is required in PF cells, transgenic cell lines were constructed using a head-to-head promoter-inducible RNAi system that is available in *T. brucei* via the vector p2T7i (28). This system allows tet-inducible expression of specific target dsRNA in PF 29-13 cells engineered to express T7 polymerase and the tet repressor. RNAi down-regulation of TbZC3H20 was confirmed using Western analysis with the anti-peptide antibody to TbZC3H20 (Fig. 2*A*). This revealed a reduction in TbZC3H20 protein to undetectable levels after RNAi induction. qPCR comparing cDNA prepared from cell lines induced with tet for 24 h with those grown in the absence of tet also confirmed down-regulation of TbZC3H20 RNA (Fig. 2*B*). β-Tubulin was used as a standard, and both β-tubulin and TbZC3H20 products were normalized to 18 S rRNA. This analysis indicated that the induced PF TbZC3H20 RNAi cells had depleted TbZC3H20 mRNA greater than 10-fold, whereas β-tubulin levels remained unaffected. Thus, specific down-regulation of TbZC3H20 after RNAi induction with tet was confirmed at both the RNA and protein levels. (Fig. 2, *A* and *B*).

RNAi of TbZC3H20 in PF parasites induced a growth defect (Fig. 2*C*), whereas morphology and cell cycle status were not significantly affected (not shown). TbZC3H20 PF RNAi cells grew normally for 3 days, then over the following 7 days growth was significantly reduced (Fig. 2*C*), suggesting TbZC3H20 may be essential in PF *T. brucei*.

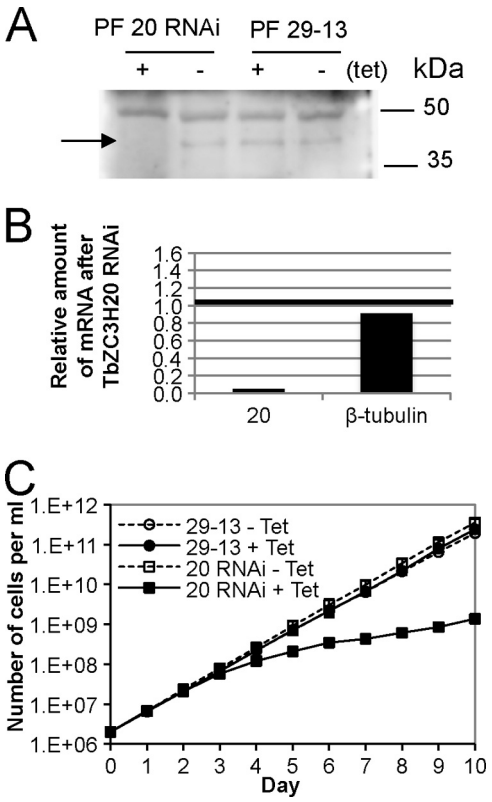

FIGURE 2. **TbZC3H20 down-regulation reduces growth in PF *T. brucei*.** *A*, the blot shows Western analysis using the anti-peptide antibody to TbZC3H20 on protein samples from PF TbZC3H20 RNAi grown in the presence (+) or absence (−) of tet and the parental cell lines treated similarly (PF29-13). The *arrow* points to PF 20 RNAi and shows the absence of detectable amounts of TbZC3H20. *B*, the graph shows the relative mRNA amount of TbZC3H20 after qPCR analysis on samples from the PF TbZC3H20 RNAi cell line 24 h after induction with tet. The abundance of the TbZC3H20 and β-tubulin mRNA from perturbed cells is shown relative to control (uninduced) cells. RNA levels are normalized to 18 S rRNA. The *thick black line* at 1 indicates no relative change in mRNA level, with anything below this line representing a decrease in mRNA levels. *C*, growth analysis shows the cumulative counts of the PF TbZC3H20 RNAi cells over 10 days. PF TbZC3H20 RNAi cells are shown by *square symbols*, whereas 29-13 cells, the parental cell line used for PF RNAi experiments, are shown with *circle symbols*. Uninduced cells (−*tet*) are shown as *dashed lines*, and *unfilled symbols* induced cells (+tet) are *solid lines with filled symbols*.

TbZC3H20 RNAi Alters the mRNA Abundance of a Small Number of Genes in PF T. brucei—To determine genes with altered levels of mRNA after depletion of TbZC3H20, the PF TbZC3H20 RNAi cells were grown with and without tet, and RNA was prepared 2 days post-induction, before any growth defect. Microarray analysis was performed on three biological replicates. Three probes (where possible) for each of the 9344 unique putative coding sequences in the *T. brucei* genome are included on each of the arrays, and the -fold change in mRNA levels for each probe on each array is shown in the supplemental Array 1, 2, and 3 data files. Only 12 different genes had changes in mRNA levels of >2-fold for at least one probe across all 3 array replicates (Table 1). This limited transcriptome response to a cellular perturbation is a feature consistent with other microarray experiments conducted in *T. brucei* (38). Thus, TbZC3H20 down-regulation did not elicit a great change in the *T. brucei* transcriptome as only 12 alterations in mRNA levels >2-fold were observed.

MCP12 and a Trans-sialidase (TS-like E) Are Stabilized in PF T. brucei—ZC3H proteins are reported to influence gene expression via a mechanism involving RNA binding and destabilization of the target transcript (20). To assess whether mRNA abundance of the transcripts putatively regulated by TbZC3H20 (Table 1) are altered by protein factors, PF parasites were incubated for 4 h in the presence or absence of cycloheximide, a known inhibitor of protein synthesis. Specifically, PF RNA was prepared from wild type cells grown in the presence of cycloheximide for 1, 2, and 4 h. Samples of RNA were examined using Northern analysis with a probe specific to each of the genes up-regulated (*top* of Fig. 3*A*) or down-regulated (*bottom* of Fig. 3*A*) in the PF TbZC3H20 RNAi cell line (microarray data, Table 1). Samples at time 0 and 4 h in the absence of cycloheximide were also analyzed to reveal steady state levels, and actin levels were used as a control. The AAT, HSP70LP, META1, and GRESAG4 did not have levels clearly altered by cycloheximide treatment. GTE1 and HP8.510 levels were reduced in 4-h-cycloheximide-treated samples, whereas HP5.4020 level was clearly increased. These are inconsistent with the changes in mRNA seen in the PF TbZC3H20 RNAi microarrays if TbZC3H20 directly regulates the abundance of these transcripts. PHAP and PAG4 were up-regulated in the PF TbZC3H20 RNAi microarrays and showed a cycloheximide pattern consistent with destabilization by a protein factor in PF parasites (Fig. 3*A*). The SA-C mRNA level at the 4-h treatment with cycloheximide was not significantly altered from both untreated samples (0 and 4 h), suggesting protein factors may or may not be involved in regulating the abundance of this mRNA in PF *T. brucei*. TS-like E and MCP12 were down-regulated in the PF TbZC3H20 RNAi microarrays and were subject to a clear reduction in mRNA level after treatment with cycloheximide (Fig. 3*A*). Cellular differentiation is critical for *T. brucei* survival, and we recognized that both MCP12 and TS-like E have previously been reported to be developmentally regulated PF-enriched transcripts (12, 39). To confirm that MCP12 and TS-like E were PF-enriched, BF and PF RNA samples were prepared and probed for the level of each mRNA (Fig. 3*B*). This showed that MCP12 and TS-like E are PF-enriched transcripts, supporting previously published data. Thus, TbZC3H20 depletion from PF *T. brucei* reduces MCP12 and TS-like E mRNA level (Table 1), and Northern analyses (Fig. 3) confirm that these two developmentally regulated transcripts are stabilized in PF *T. brucei* by a protein factor. Therefore, this suggests that TS-like E and MCP12 transcript levels may be specifically stabilized by TbZC3H20. This differs from the destabilization mechanism of regulating mRNA abundance that has previously been reported for ZC3Hs and warranted further investigation.

TbZC3H20 Stabilizes MCP12 and TS-like E mRNAs in PF T. brucei—Having confirmed that MCP12 and TS-like E are life cycle stage-regulated transcripts that are stabilized in PF cells and that their mRNA abundance is reduced after depletion of TbZC3H20 from PF *T. brucei*, Northern analyses were performed to assess whether TbZC3H20 down-regulation in PF cells influenced the mRNA half-life of MCP12 and TS-like E. RNA and protein samples were prepared from PF TbZC3H20 RNAi *T. brucei* after incubation with and without tet for 48 h. At 48 h the protein and mRNA levels of TbZC3H20 were sig-

TABLE 1

Summary of the microarray analysis of PF TbZC3H20 RNAi cells

Genes with altered levels of RNA >2-fold are shown up-regulated or down-regulated as a result of RNAi-mediated down-regulation of TbZC3H20 in PF cells. Signal -fold change (+ = up regulated, − = down-regulated) for each of the three arrays conducted are shown for each of the probes on the array for that specific gene. Probes that are not >2 fold across all three arrays are shown in italics.

Number	Probe	Array 1	Array 2	Array 3	Product
Up-regulated RNAs					
Tb927.8.480	1	+13.4	+2.1	+2.7	Phosphatidic acid phosphatase (PHAP)
	2	+10.2	+2.1	+2.5	
	3	+8.3	+2.5	+2.7	
Tb927.8.510	1	+10.3	+2.0	+2.0	Hypothetical protein (orphan) (HP8.510)
	2	*+6.0*	*+1.1*	*+0.6*	
	3	*+4.0*	*+1.0*	*+1.5*	
Tb09.160.3090	1	+4.6	+2.1	+3.1	Heat shock protein, HSP70-like protein (HSP70LP)
	2	*+5.1*	*+1.6*	*+2.5*	
	3	*+4.3*	*+1.8*	*+2.1*	
Tb10.6k15.0050/	1	+13.7	+2.6	+3.5	Procyclin-associated gene 5 (PAG5)
	2	+9.2	+2.2	+4.0	
	3	+9.6	+2.3	+4.0	
0060/	1	+11.6	+2.7	+3.3	Procyclin-associated gene 2 (PAG2)
	2	+8.9	+2.6	+3.8	
	3	+9.3	+3.0	+4.1	
0070/	1	+10.9	+2.4	+3.9	Procyclin-associated gene 4 (PAG4)
	2	*+8.8*	*+1.8*	*+2.4*	
	3	*+10.2*	*+1.9*	*+2.2*	
3540	1	+4.9	+2.1	+3.1	Procyclin-associated gene 1 (PAG1)
	2	*+6.4*	*+1.9*	*+2.3*	
	3	*+6.8*	*+1.9*	*+2.1*	
Tb10.6k15.2030	1	+6.5	+2.2	+2.8	Glucose transporter 1E (GTE1)
	2	*+2.3*	*+0.6*	*+0.9*	
Tb11.01.7590/	1	+6.3	+2.2	+2.7	Amino acid transporter (AAT)
	2	+6.8	+2.7	+3.7	
	3	*+6.7*	*+1.7*	*+2.1*	
7600	1	+8.6	+3.1	+3.5	Amino acid transporter
	1(2)	+9.0	+3.1	+3.8	
	2	+6.1	+2.6	+2.9	
	3	+9.0	+2.2	+2.7	
	4	*+9.6*	*+1.9*	*+2.4*	
Down-regulated RNAs					
Tb927.5.2160/	1	−3.1	−6.9	−7.4	Hypothetical protein, conserved (META1)
	2	−4.1	−7.5	−8.5	
2170/	1	−3.1	−6.8	−8.1	
2260	1	−3.7	−9.5	−10.9	
Tb927.5.4020	1	−2.9	−5.8	−3.7	Hypothetical protein (orphan) (HP5.4020)
	2	−3.3	−6	−4.3	
	3	−2.9	−6.8	−3.8	
Tb927.5.440	1	−2.1	−4.4	−3.1	Hypothetical protein, conserved *Trans*-sialidase (TS-like E)
	2	*−1.8*	*−2.9*	*−2.1*	
	3	*−1.4*	*−4*	*−3.1*	
Tb927.8.7340	1	−2.1	−2.6	−2.3	*Trans*-sialidase, neuraminidase (SA C)
	2	*−1.9*	*−2.8*	*−2.2*	
	3	*−1.8*	*−2.8*	*−2.6*	
Tb10.389.0690	1	−3.1	−3.2	−2.2	Mitochondrial carrier protein (MCP12)
	2	−2.6	−4.3	−2.5	
	3	−2.7	−3.7	−2.5	
Tb11.02.3740	1	−2.4	−5.8	−4.2	Receptor-type adenylate cyclase (GRESAG4)
	2	−2.3	−5	−4.1	
	3	*−0.7*	*−4*	*−4.7*	

nificantly reduced with no obvious growth defects evident in the cells (Fig. 2, *A–C*). PF TbZC3H20 RNAi induction was then followed by treatment with the transcriptional inhibitor actinomycin D for 0, 1, 2, or 4 h to allow the turnover of transcripts to be observed in RNA samples from PF *T. brucei* with or without induction of TbZC3H20 RNAi. A representative Northern analysis is shown for mRNA levels of MCP12 and TS-like E (Fig. 4*A*). Actin is used as a control. Three biological replicates were performed, and the level of mRNA for MCP12, TS-like E, and actin was determined using densitometry on Northern analyses of the actinomycin D-treated samples (Fig. 4*B*). The mRNA half-life of MCP12, TS-like E, and actin were calculated from the plots of cells induced for RNAi of TbZC3H20 and compared with those of uninduced cells over the 4-h treatment with actinomycin D (Fig. 4*B*). This indicated no significant difference in actin mRNA half-life (66 *versus* 54 min) and showed a significant difference between MCP12 and TS-like E mRNA half-lives (>240 *versus* 114 min and >240 *versus* 144 min, respectively). Thus, these two transcripts are turned over more rapidly in the absence of TbZC3H20, indicating that TbZC3H20 stabilizes MCP12 and TS-like E mRNA in PF *T. brucei*.

TbZC3H20 Binds MCP12 and TS-like E mRNA—Having observed that MCP12 and TS-like E transcripts had shorter half-lives in the absence of TbZC3H20 in PF *T. brucei,* experiments were conducted to determine whether TbZC3H20 is capable of binding these target mRNAs. Immunoprecipitation experiments with the TbZC3H20 anti-peptide antibody proved

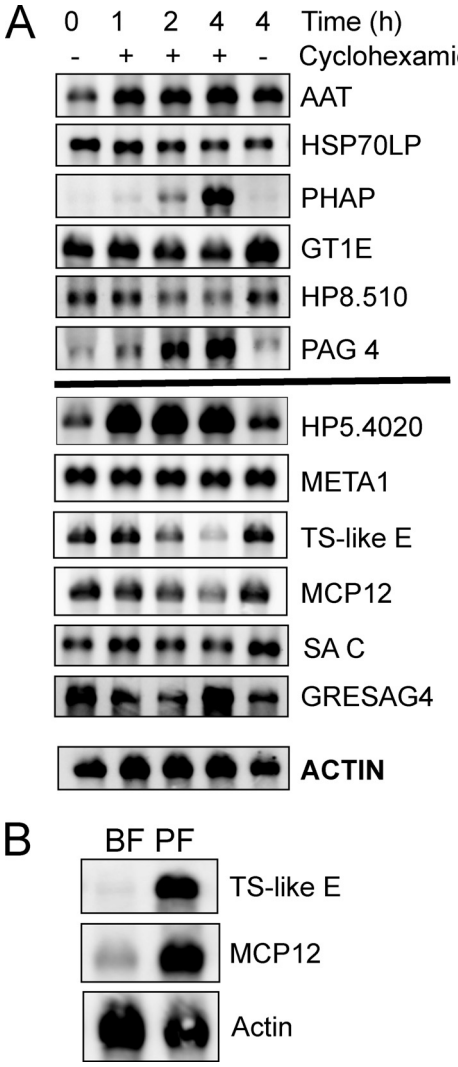

FIGURE 3. **MCP12 and TS-like E have reduced mRNA levels after treatment with cycloheximide and are PF-enriched transcripts.** *A*, shown are Northern blots of mRNA levels from PF *T. brucei* cells treated (+) or not (−) with the translational inhibitor cycloheximide where RNA was isolated at 0, 1, 2, and 4 h. *Panels above the thick black line* show Northern analysis for each specific transcript up-regulated in the PF TbZC3H20 RNAi microarray experiment. *Panels below the thick black line* show Northern analysis for each specific transcript down-regulated in the PF TbZC3H20 RNAi microarray experiment. Actin transcript levels are shown as a control. Abbreviations used for gene names are as in Table 1. *B*, Northern blots of mRNA levels from BF and PF *T. brucei* confirm that the levels of mRNA for MCP12 and TS-like E are enriched in PF compared with BF *T. brucei*. Actin transcript levels are shown as a control.

unsuccessful. Thus, a tandem affinity purification (TAP) tagging approach, which has proved useful in trypanosomes, was employed (40). PF 29-13 cells were engineered with a TAP-20 construct stably integrated and the TAP-20 protein purified from cells using IgG and calmodulin columns. RNA that co-precipitated with TAP-20 was reverse-transcribed, and cDNA was then subjected to PCR with primers specific for MCP12 and TS-like E. Control RT-PCR was also performed with actin and tubulin. The TAP tagging procedure was also performed with TbZC3H36, another member of the TbZC3H family, as a control for TAP-20-specific RNA binding. TAP RT-PCR results show that both actin and tubulin did not bind TAP-20 (or TAP-36) (Fig. 5*A*). However, MCP12 and TS-like E produced a PCR product of the correct predicted size that was only

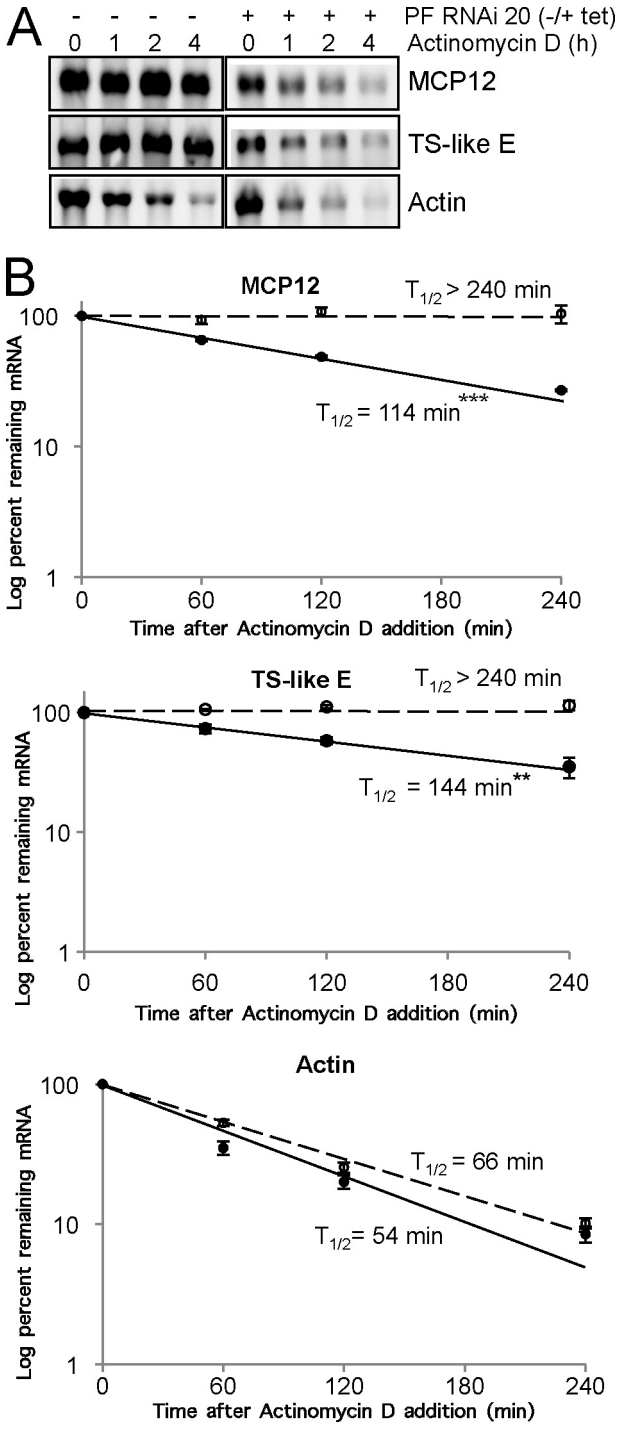

FIGURE 4. **TbZC3H20 stabilizes the MCP12 and TS-like E mRNAs.** *A*, shown are representative Northern blots of PF RNA, hybridized with probes to MCP12 and TS-like E, from cells treated with the transcriptional inhibitor actinomycin D. RNA was isolated at 0, 1, 2, and 4 h from PF TbZC3H20 RNAi cells grown in the presence of tet (+) or without tet (−). Actin is used as a control. *B*, graphs show the signal quantification (mean) from three biological replicates of Northern analysis as described for the PF TbZC3H20 RNAi actinomycin treated cell experiment above in *A* for MCP12 and TS-like E. Each data point represents the level of mRNA with respect to its abundance before the addition of actinomycin (0 h), which is shown as 100%. PF TbZC3H20 RNAi-induced samples (+) are shown as *filled circles with a solid line*, whereas uninduced samples are *unfilled circles with dashed lines*. Actin is shown as a control. *Error bars* show the S.D. Student's *t* tests indicate no significant difference in the actin samples, whereas the MCP12 and TS-like E are significant at $p < 0.001$ (***).

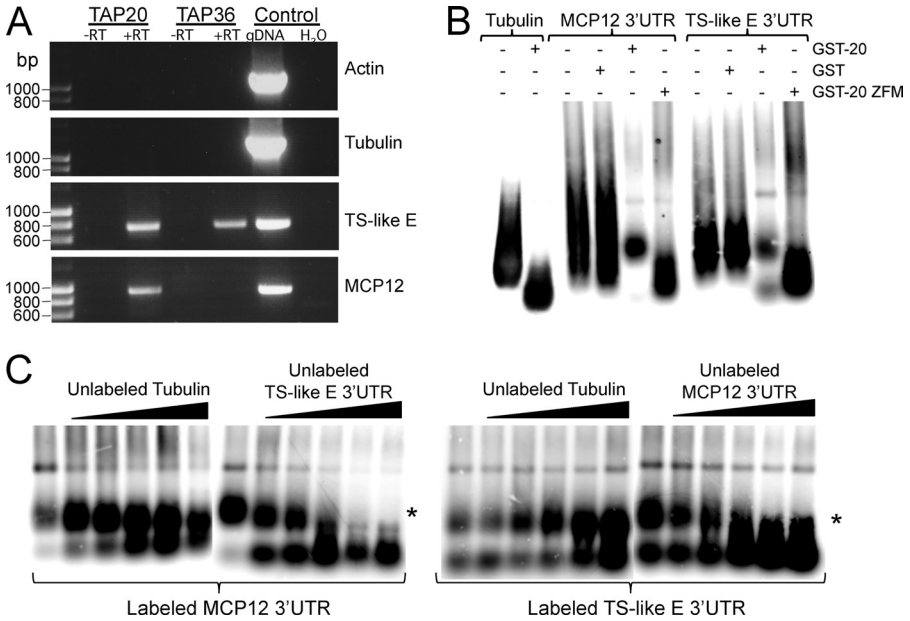

FIGURE 5. **TbZC3H20 binds MCP12 and TS-like E RNA.** *A*, TAP-tagged TbZC3H20 (TAP-20) and TbZC3H36 (TAP-36) were used to co-precipitate RNA in PF *T. brucei*. RNA derived from each TAP experiment was converted to cDNA in one reaction (+*RT*) and the reverse transcriptase was omitted from another (−*RT*). PCR was performed on each sample with primers specific for actin, tubulin, MCP12, and TS-like E as indicated for each panel. PCR reactions with each primer set were also conducted on genomic DNA (*gDNA*) as a positive control. The −RT reactions are a control for genomic DNA contamination. PCR amplicons of the correct predicted size were obtained in the TAP-20 +RT samples only (MCP12 = 891 bp and TS-like E = 728 bp). *B*, shown is an RNA electrophoretic mobility shift assay of GST-TbZC3H20 with MCP12 or TS-like E 3′-UTR RNAs. Target RNAs are digoxigenin-labeled 3′-UTRs of MCP12 (1393 nucleotides) or TS-like E (615 nucleotides). For each reaction, 5 ng of RNA was incubated in the absence of protein, with 500 nM GST-TbZC3H20 (GST-20) or with 500 nM of GST alone (GST) as a control, to exclude nonspecific electrostatic interactions. As a control for the specificity of RNA binding, 5 ng of labeled tubulin RNA (1354 nucleotides) was incubated with or without 500 nM GST-TbZC3H20. The TbZC3H20 CCCH zinc finger motif mutant (GST-20 ZFM) has the third critical cysteine residue of both motifs substituted for an alanine residue (CCAH). MCP12 or TS-like E RNAs (5 ng) were also incubated with GST-20 ZFM (500 nM). This indicated ZC3H motif of TbZC3H20 involvement in direct binding to MCP12 and TS-like E 3′-UTR RNA. *C*, competition RNA electrophoretic mobility shift assays are shown. Labeled MCP12 RNA (5 ng) is shown on the *left panels* with increasing ratios (1:1, 1:5, 1:25, 1:100, and 1:200 indicated by the *solid triangle*) of unlabeled tubulin or TS-like E RNAs as competitors. Labeled TS-like E RNA (5 ng) is shown on the *right panels* with increasing ratios (1:1, 1:5, 1:25, 1:100 and 1:200 indicated by the *solid triangle*) of unlabeled tubulin or MCP12 RNAs as competitors. Each reaction was incubated with 500 nM GST-TbZC3H20. The *first lane of each panel* contains no competitor RNA. The asterisk (*) indicates the position of the electrophoretic mobility shifted RNA.

present in the TAP-20-co-precipitated sample for MCP12, whereas products for TS-like E were obtained in both TAP-20 and TAP-36 samples (Fig. 5*A*). Reverse transcriptase minus (RT−) TAP-20-co-precipitated RNA did not show PCR amplification products, ruling out genomic DNA contamination. The presence of a TS-like E PCR product in the TAP-36 sample suggests that binding specificity for ZC3Hs may be more general for this mRNA. Importantly, this analysis provides evidence that TbZC3H20 is capable of binding to MCP12 and TS-like E mRNA.

To assess the capacity of TbZC3H20 to directly bind the target mRNAs, MCP12 and TS-like E, an RNA electrophoretic mobility shift assay was performed. Digoxigenin-labeled RNA was *in vitro* transcribed from the 3′-UTRs of tubulin, MCP, and TS-like E and used in an *in vitro* binding reaction in the absence or presence of recombinant GST-TbZC3H20 (500 nM). Labeled RNAs were also incubated with GST alone (500 nM) as a control. Binding reactions were electrophoresed on agarose gels and transferred to a nylon membrane, and RNA was detected using chemiluminescence (Fig. 5*B*). In the absence of GST-TbZC3H20 or in the presence of GST alone, the MCP12 and TS-like E 3′-UTR RNA mobility is not affected, verifying that the presence of the GST tag alone does not confer binding to either MCP12 or TS-like E 3′-UTR RNA. GST-TbZC3H20 protein (500 nM) resulted in an RNA mobility shift for both MCP12 and TS-like E target RNAs but not for the tubulin control RNA (Fig. 5*B*). This shows TbZC3H20 is capable of directly binding to the 3′-UTRs of MCP12 and TS-like E. Additionally, to show the involvement of the ZC3H motifs within TbZC3H20 in binding directly to target transcripts, the third critical cysteine residue of both motifs were mutated to alanine, and recombinant TbZC3H20 CCCH zinc finger motif mutant (GST-20 ZFM) protein was used in an electrophoretic mobility shift assay with MCP12 and TS-like E 3′-UTR mRNAs (Fig. 5*B*). This analysis revealed that the GST-20 ZFM mutant protein was unable to bind MCP12 or TS-like E 3′-UTR mRNAs, suggesting the ZC3H motifs of TbZC3H20 are necessary for direct binding.

Furthermore, competition assays were carried out using increasing concentrations of unlabeled tubulin, MCP12, or TS-like E 3′-UTR RNA in the electrophoretic mobility shift assays with GST-TbZC3H20 (500 nM) as shown in Fig. 5*C*. Specifically, labeled MCP12 RNA was competed with unlabeled tubulin or TS-like E RNAs (*left side panels,* Fig. 5*C*), and labeled TS-like E RNA was competed with unlabeled tubulin or MCP12 RNAs (*right side panels*, Fig. 5*C*). This showed a reduction of detectable GST-TbZC3H20 bound RNAs when competition was with MCP12 or TS-like E but no reduction in shifted RNA when tubulin was used as the competitor. This confirmed the selectivity of GST-TbZC3H20 for binding MCP12 and TS-like E 3′-UTR RNA.

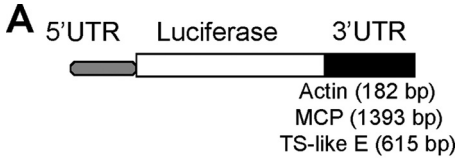

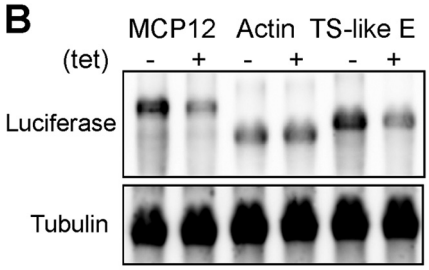

C

	MCP12	Actin	TS-like E
RNAi 20 -	100	100	100
RNAi 20 +	55 ± 1.2	110 ± 2.9	44 ± 5.3
Difference	45 ± 1.2	10 ± 2.9	56 ± 5.3
Significance	p < 0.001		p < 0.001

FIGURE 6. **The 3′-UTR of MCP12 and TS-like E contain sequence elements capable of regulating a luciferase reporter gene in a TbZC3H20-dependent manner.** *A*, shown is a schematic diagram illustrating the reporter system used to determine whether the MCP12 and TS-like E 3′-UTRs contain sequence elements capable of regulating expression of a luciferase reporter gene. The system allowed for tet-inducible down-regulation of TbZC3H20 to determine whether 3′-UTR regulation of the reporter was TbZC3H20-dependent. *B*, Northern analysis shows the level of luciferase mRNA in each reporter construct with either MCP12, TS-like E, or actin 3′-UTR sequence. TbZC3H20 expression is down-regulated in these cell lines using tet (+) and compared with uninduced cells (−). *C*, shown is the average percentage level of each luciferase mRNA in each reporter construct from three biological replicates of TbZC3H20 RNAi cells grown in the presence (+) or absence (−) of tet. Uninduced cell lines for each luciferase reporter cell lines are taken as a 100% level of mRNA. The difference in induced *versus* uninduced samples is tabulated. The mean difference (±S.D.) in MCP12 and TS-like E levels was then compared with the difference in actin levels and subjected to Student's *t* test, and both were found to be significant at $p < 0.001$ (tabulated in Fig. 6*C*).

MCP12 and TS-like E Are Regulated via Elements in Their 3′-UTR—Previous studies of ZC3Hs have shown them to destabilize target mRNAs via sequences in the 3′-UTR of target transcripts (19, 41). To determine whether MCP12 and TS-like E are TbZC3H20-regulated through sequence elements in their 3′-UTRs, a luciferase reporter was employed (Fig. 6*A*, and the sequences downstream of the MCP12 and TS-like E stop codon to the next coding region in the genome are in supplemental Fig. 2). The reporter constructs were transfected (stably integrated) into the PF TbZC3H20 RNAi cell line and induced or uninduced with tet to mediate TbZC3H20 RNAi. The luciferase reporter with an actin 3′-UTR was used as a control. A representative blot of luciferase RNA level from each 3′-UTR reporter construct (with and without tet) indicates a change in the level of MCP12 and TS-like E when TbZC3H20 is down-regulated, whereas actin levels remain unchanged (Fig. 6*B*). The percentage difference in luciferase mRNA levels (Northern blots subjected to densitometry) from induced and uninduced PF TbZC3H20 RNAi cells for each of the luciferase 3′-UTR constructs is shown in Fig. 6*C*. A significant reduction was observed in the PF TbZC3H20 RNAi cells induced with tet for the luciferase reporter with either MCP12 or TS-like E 3′-UTRs, whereas the level of luciferase mRNA with the actin 3′-UTR remained relatively unchanged (Fig. 6*C*). Collectively, these data demonstrate MCP12 and TS-like E transcripts are specifically stabilized through sequence elements in their 3′-UTR in a TbZC3H20-dependent manner.

DISCUSSION

Reports of post-transcriptional control mechanisms of regulating gene expression, including mRNA turnover, are rapidly increasing. This work characterizes TbZC3H20, a member of the ZC3H family of RBPs, from *T. brucei*. TbZC3H20 was shown to be capable of binding RNA *in vitro* and *in vivo*, and Western analysis with an anti-peptide antibody to TbZC3H20 indicated higher levels in PF compared with BF *T. brucei*. RNAi depletion indicated TbZC3H20 was required for normal growth in PF parasites. Microarray experiments show PF cells depleted of TbZC3H20 changed the mRNA level of only 12 different genes >2-fold. PF cells treated with an inhibitor of protein synthesis revealed that two transcripts putatively regulated by TbZC3H20 (MCP12 and TS-like E) were stabilized in PF cells, and Northern analysis confirmed MCP12 and TS-like E are PF-enriched mRNAs. TbZC3H20-dependent regulation of MCP12 and TS-like E mRNA half-life was confirmed by actinomycin D inhibitor studies and Northern analysis. TbZC3H20 binding of MCP12 and TS-like E was demonstrated via TAP-tagging RT-PCR experiments. MCP12 and TS-like E, both, contained 3′-UTR sequence elements capable of regulating reporter gene expression in a TbZC3H20-dependent manner. The mitochondrial carrier protein, MCP12, and the *trans*-sialidase TS-like E, therefore, represent specific target transcripts regulated via stabilization by TbZC3H20 in PF *T. brucei*.

ZC3Hs are known as negative regulators of gene expression (42), and to the best of our knowledge this is the first report of a ZC3H demonstrating an ability to stabilize a specific target mRNA. This has implications for the mechanism utilized by ZC3Hs to control mRNA abundance. Destabilization involves promoting exonucleolytic activity for a target transcript and recruiting either the 5′-3′ or 3′-5′ nucleolytic degradation machinery (43). Additionally, some RBPs, for example ZC3H12a, have been found to possess RNase activity as part of a destabilizing mechanism (44). Deadenylation is integral to mRNA degradation, and the ZC3H C3H-4 has been discovered to recruit the CCR4 deadenylase to specific mRNAs (45). These findings all support a role for ZC3Hs in destabilizing target mRNAs. The RRM family of RBPs has been shown to have roles in stabilizing target mRNAs, most notably HuR and AUF1 (3), but until now ZC3Hs have not. This work on TbZC3H20, demonstrating the involvement of a ZC3H in stabilization of target mRNA abundance, suggests that poly(A)-binding protein (PABP) and/or translational initiation factors must also be able to be recruited by ZC3Hs, as this is how mRNA is normally protected from deadenylation and degradation (43). ZC3Hs have relatively recently been shown to bind poly(A) (46), suggesting a route for ZC3Hs to stabilize target mRNA.

The $C_{7-8}C_5C_3H$ motif-containing ZC3Hs have to date been reported to operate via class II AREs in the 3′UTR of targeted transcripts using a UUAUUUAUU consensus nonamer (Ref. 47; for a review of the ARE classifications, see Ref. 3.) MCP12

and TS-like E are regulated via elements in their 3′-UTRs, but investigation of these 3′-UTR sequences (supplemental Fig. 2) reveals they do not contain the consensus nonamer (UUAUUUAUU) that is characteristic of the ARE targets of previously studied ZC3Hs (48). However, the 3′-UTR of TS-like E contains several AUUUA pentamers and U-rich regions that define class I AREs (supplemental Fig. 2). The MCP12 3′-UTR does not contain class I or II AREs, but does have several U-rich regions lacking an AUUUA pentamer, a feature of the poorly defined class III ARE. One possibility is that ZC3Hs are capable of recognizing all three ARE classes and thereby destabilize or stabilize target transcripts. Alternatively, studies have identified GU-rich sequences (GREs) that may also act as mRNA stability elements (49). GRE-like sequences are contained in the TS-like E and MCP12 3′-UTRs (supplemental Fig. 2), and these speculatively represent a route to ARE-independent regulation of these transcripts.

MCP12 and TS-like E have at least 2-fold enriched mRNA levels in PF compared with BF *T. brucei* (12). Approximately a third of the transcripts enriched in PF parasites harbor a UAUUUUUU sequence in the 3′-UTR that acts as a destabilization element in BF parasites, thus giving rise to a comparative increase in levels of that specific mRNA in PF parasites (50). This UAUUUUUU sequence is present in the 3′-UTR of TS-like E but absent from MCP12 (supplemental Fig. 2). It is not surprising that the 3′-UTR of MCP12 does not contain this *cis* element, as its mRNA levels are regulated via TbZC3H20-dependent stabilization in PF cells. The fact that TS-like E is stabilized by TbZC3H20 but does harbor the UAUUUUU suggests that other *trans*-acting factors in BF parasites may also contribute to TS-like E differential expression or that the element is present by chance. With only two defined target transcripts (MCP12 and TS-like E) for TbZC3H20, it is difficult to identify if common sequence elements exist in the 3′-UTRs of MCP12 and TS-like E by using oligomer search tools or RNA-fold prediction programs, as similarities are purely speculative with such a limited test set. Extensive mapping of the MCP12 and TS-like E 3′-UTR is useful in further work to find more precise regulatory *cis* elements, which may display similar sequence or secondary structural characteristics or be completely novel sequence elements.

There are several key differences between how energy requirements are met in BF and PF parasites (51). In BF parasites, ATP is generated exclusively via the glycolytic pathway, and the mitochondria are relatively inactive. In PF parasites the mitochondrion is active, and cells obtain most of their energy through mitochondrial catabolism of proline (51). MCPs are important in this process, and *T. brucei* contains 24 members from this protein family (39). MCP12 encodes the putative malate/oxoglutarate transporter, and comparative genomics suggest the MCP12 gene encodes the only oxoglutarate and dicarboxylate carrier protein in the *T. brucei* genome (39). Malate and oxoglutarate are important in PF *T. brucei* as intermediates of energy metabolism and potentially in maintaining cellular redox balance via the isocitrate/oxoglutarate shuttle (39). It is, therefore, a significant finding that TbZC3H20 regulates the stability of the MCP12 mRNA as a mechanism to ensure differential expression during the parasites life cycle. This discovery is more broadly significant, as previous ZC3H investigations have demonstrated an involvement in regulating the stability of specific immune response genes (21, 42) or virus proliferation (52), but this work is the first to demonstrate regulation of a gene encoding a mitochondrial protein.

Trypanosomes are unable to synthesize sialic acid, but PF *T. brucei* is able to utilize sialylated glycoconjugates present in the fly midgut via separate sialidase and *trans*-sialidase enzymes on its surface membrane (53). TS-like E represents a divergent *trans*-sialidase gene, which has a PF-enriched transcript. TS-like E *trans*-sialidase is one of six genes in the *T. brucei* genome encoding proteins with a putative *trans*-sialidase function. The regulation of TS-like E by TbZC3H20 may assist in understanding how sialic acid levels are controlled. Because of the importance of *trans*-sialidase/sialidase activity in maintaining the glycosylphosphatidylinositol-anchored proteins at the surface of the trypanosome, these represent potential vaccine targets in trypanosomes (54).

Although many RBPs are conserved across eukaryotic organisms, TbZC3H20 has no identifiable homologues and is required for normal growth in PF *T. brucei*. Thus, both the genes regulated by TbZC3H20 and TbZC3H20 itself may represent good anti-trypanosome drug targets. Significantly, this work shows TbZC3H20 can regulate trypanosome gene expression via mRNA stabilization, a mechanism not previously demonstrated for ZC3H RBPs. Future investigations into ZC3Hs and other RBPs acting to regulate mRNA levels of specific target genes in trypanosomes should also prove enlightening.

Acknowledgments—We thank Ken Stuart for the kind gift of pLEW79-TAP plasmid. We are extremely grateful to Antonio Estevez for providing the pGR86 and 108 plasmids.

REFERENCES

1. Mata, J., Marguerat, S., and Bähler, J. (2005) *Trends Biochem. Sci.* **30,** 506–514
2. Glisovic, T., Bachorik, J. L., Yong, J., and Dreyfuss, G. (2008) *FEBS Lett.* **582,** 1977–1986
3. Barreau, C., Paillard, L., and Osborne, H. B. (2005) *Nucleic Acids Res.* **33,** 7138–7150
4. Embley, T. M., and Martin, W. (2006) *Nature* **440,** 623–630
5. Berriman, M., Ghedin, E., Hertz-Fowler, C., Blandin, G., Renauld, H., Bartholomeu, D. C., Lennard, N. J., Caler, E., Hamlin, N. E., Haas, B., Böhme, U., Hannick, L., Aslett, M. A., Shallom, J., Marcello, L., Hou, L., Wickstead, B., Alsmark, U. C., Arrowsmith, C., Atkin, R. J., Barron, A. J., Bringaud, F., Brooks, K., Carrington, M., Cherevach, I., Chillingworth, T. J., Churcher, C., Clark, L. N., Corton, C. H., Cronin, A., Davies, R. M., Doggett, J., Djikeng, A., Feldblyum, T., Field, M. C., Fraser, A., Goodhead, I., Hance, Z., Harper, D., Harris, B. R., Hauser, H., Hostetler, J., Ivens, A., Jagels, K., Johnson, D., Johnson, J., Jones, K., Kerhornou, A. X., Koo, H., Larke, N., Landfear, S., Larkin, C., Leech, V., Line, A., Lord, A., Macleod, A., Mooney, P. J., Moule, S., Martin, D. M., Morgan, G. W., Mungall, K., Norbertczak, H., Ormond, D., Pai, G., Peacock, C. S., Peterson, J., Quail, M. A., Rabbinowitsch, E., Rajandream, M. A., Reitter, C., Salzberg, S. L., Sanders, M., Schobel, S., Sharp, S., Simmonds, M., Simpson, A. J., Tallon, L., Turner, C. M., Tait, A., Tivey, A. R., Van Aken, S., Walker, D., Wanless, D., Wang, S., White, B., White, O., Whitehead, S., Woodward, J., Wortman, J., Adams, M. D., Embley, T. M., Gull, K., Ullu, E., Barry, J. D., Fairlamb, A. H., Opperdoes, F., Barrell, B. G., Donelson, J. E., Hall, N., Fraser, C. M., Melville, S. E., and El-Sayed, N. M. (2005) *Science* **309,** 416–422
6. Ivens, A. C., Peacock, C. S., Worthey, E. A., Murphy, L., Aggarwal, G.,

Berriman, M., Sisk, E., Rajandream, M. A., Adlem, E., Aert, R., Anupama, A., Apostolou, Z., Attipoe, P., Bason, N., Bauser, C., Beck, A., Beverley, S. M., Bianchettin, G., Borzym, K., Bothe, G., Bruschi, C. V., Collins, M., Cadag, E., Ciarloni, L., Clayton, C., Coulson, R. M., Cronin, A., Cruz, A. K., Davies, R. M., De Gaudenzi, J., Dobson, D. E., Duesterhoeft, A., Fazelina, G., Fosker, N., Frasch, A. C., Fraser, A., Fuchs, M., Gabel, C., Goble, A., Goffeau, A., Harris, D., Hertz-Fowler, C., Hilbert, H., Horn, D., Huang, Y., Klages, S., Knights, A., Kube, M., Larke, N., Litvin, L., Lord, A., Louie, T., Marra, M., Masuy, D., Matthews, K., Michaeli, S., Mottram, J. C., Müller-Auer, S., Munden, H., Nelson, S., Norbertczak, H., Oliver, K., O'neil, S., Pentony, M., Pohl, T. M., Price, C., Purnelle, B., Quail, M. A., Rabbinowitsch, E., Reinhardt, R., Rieger, M., Rinta, J., Robben, J., Robertson, L., Ruiz, J. C., Rutter, S., Saunders, D., Schäfer, M., Schein, J., Schwartz, D. C., Seeger, K., Seyler, A., Sharp, S., Shin, H., Sivam, D., Squares, R., Squares, S., Tosato, V., Vogt, C., Volckaert, G., Wambutt, R., Warren, T., Wedler, H., Woodward, J., Zhou, S., Zimmermann, W., Smith, D. F., Blackwell, J. M., Stuart, K. D., Barrell, B., and Myler, P. J. (2005) *Science* **309,** 436–442

7. Liang, X. H., Haritan, A., Uliel, S., and Michaeli, S. (2003) *Eukaryot. Cell* **2,** 830–840
8. Clayton, C. E. (2002) *EMBO J.* **21,** 1881–1888
9. Hendriks, E., and Matthews, K. (2007) *Post-transcriptional Control of Gene Expression in African Trypansomes*, pp. 210–238, Horizon Bioscience, U.K.
10. Matthews, K. R. (2005) *J. Cell Sci.* **118,** 283–290
11. Matthews, K. R., Ellis, J. R., and Paterou, A. (2004) *Trends Parasitol.* **20,** 40–47
12. Jensen, B. C., Sivam, D., Kifer, C. T., Myler, P. J., and Parsons, M. (2009) *BMC Genomics* **10,** 482
13. Kabani, S., Fenn, K., Ross, A., Ivens, A., Smith, T. K., Ghazal, P., and Matthews, K. (2009) *BMC Genomics* **10,** 427
14. Queiroz, R., Benz, C., Fellenberg, K., Hoheisel, J. D., and Clayton, C. (2009) *BMC Genomics* **10,** 495
15. Mackay, J. P., and Crossley, M. (1998) *Trends Biochem. Sci.* **23,** 1–4
16. Brown, R. S. (2005) *Curr. Opin. Struct. Biol.* **15,** 94–98
17. Lai, W. S., Kennington, E. A., and Blackshear, P. J. (2002) *J. Biol. Chem.* **277,** 9606–9613
18. Liang, J., Wang, J., Azfer, A., Song, W., Tromp, G., Kolattukudy, P. E., and Fu, M. (2008) *J. Biol. Chem.* **283,** 6337–6346
19. Wang, D., Guo, Y., Wu, C., Yang, G., Li, Y., and Zheng, C. (2008) *BMC Genomics* **9,** 44
20. Blackshear, P. J. (2002) *Biochem. Soc. Trans.* **30,** 945–952
21. Carballo, E., Lai, W. S., and Blackshear, P. J. (1998) *Science* **281,** 1001–1005
22. Gao, G., Guo, X., and Goff, S. P. (2002) *Science* **297,** 1703–1706
23. Reese, K. J., Dunn, M. A., Waddle, J. A., and Seydoux, G. (2000) *Mol. Cell* **6,** 445–455
24. Hendriks, E. F., and Matthews, K. R. (2005) *Mol. Microbiol.* **57,** 706–716
25. Hendriks, E. F., Robinson, D. R., Hinkins, M., and Matthews, K. R. (2001) *EMBO J.* **20,** 6700–6711
26. Paterou, A., Walrad, P., Craddy, P., Fenn, K., and Matthews, K. (2006) *J. Biol. Chem.* **281,** 39002–39013
27. Walrad, P., Paterou, A., Acosta-Serrano, A., and Matthews, K. R. (2009) *PLoS Pathog.* **5,** e1000317
28. LaCount, D. J., Barrett, B., and Donelson, J. E. (2002) *J. Biol. Chem.* **277,** 17580–17588
29. Panigrahi, A. K., Schnaufer, A., Ernst, N. L., Wang, B., Carmean, N., Salavati, R., and Stuart, K. (2003) *RNA* **9,** 484–492
30. Estévez, A. M. (2008) *Nucleic Acids Res.* **36,** 4573–4586
31. Wirtz, E., Leal, S., Ochatt, C., and Cross, G. A. (1999) *Mol. Biochem. Parasitol.* **99,** 89–101
32. Hendriks, E. F., Abdul-Razak, A., and Matthews, K. R. (2003) *J. Biol. Chem.* **278,** 26870–26878
33. Carnes, J., Trotter, J. R., Ernst, N. L., Steinberg, A., and Stuart, K. (2005) *Proc. Natl. Acad. Sci. U.S.A.* **102,** 16614–16619
34. Pfaffl, M. W. (2001) *Nucleic Acids Res.* **29,** e45
35. Ramakers, C., Ruijter, J. M., Deprez, R. H., and Moorman, A. F. (2003) *Neurosci. Lett.* **339,** 62–66
36. Hertz-Fowler, C., Peacock, C. S., Wood, V., Aslett, M., Kerhornou, A., Mooney, P., Tivey, A., Berriman, M., Hall, N., Rutherford, K., Parkhill, J., Ivens, A. C., Rajandream, M. A., and Barrell, B. (2004) *Nucleic Acids Res.* **32,** D339–D343
37. Kramer, S., Kimblin, N. C., and Carrington, M. (2010) *BMC Genomics* **11,** 283
38. Koumandou, V. L., Natesan, S. K., Sergeenko, T., and Field, M. C. (2008) *BMC Genomics* **9,** 298
39. Colasante, C., Peña Diaz, P., Clayton, C., and Voncken, F. (2009) *Mol. Biochem. Parasitol.* **167,** 104–117
40. Panigrahi, A. K., Allen, T. E., Stuart, K., Haynes, P. A., and Gygi, S. P. (2003) *J. Am. Soc. Mass. Spectrom.* **14,** 728–735
41. Lai, W. S., Carballo, E., Strum, J. R., Kennington, E. A., Phillips, R. S., and Blackshear, P. J. (1999) *Mol. Cell. Biol.* **19,** 4311–4323
42. Lai, W. S., Parker, J. S., Grissom, S. F., Stumpo, D. J., and Blackshear, P. J. (2006) *Mol. Cell. Biol.* **26,** 9196–9208
43. Parker, R., and Song, H. (2004) *Nat. Struct. Mol. Biol.* **11,** 121–127
44. Matsushita, K., Takeuchi, O., Standley, D. M., Kumagai, Y., Kawagoe, T., Miyake, T., Satoh, T., Kato, H., Tsujimura, T., Nakamura, H., and Akira, S. (2009) *Nature* **458,** 1185–1190
45. Belloc, E., and Méndez, R. (2008) *Nature* **452,** 1017–1021
46. Kelly, S. M., Pabit, S. A., Kitchen, C. M., Guo, P., Marfatia, K. A., Murphy, T. J., Corbett, A. H., and Berland, K. M. (2007) *Proc. Natl. Acad. Sci. U.S.A.* **104,** 12306–12311
47. Lai, W. S., Carrick, D. M., and Blackshear, P. J. (2005) *J. Biol. Chem.* **280,** 34365–34377
48. Cuthbertson, B. J., Liao, Y., Birnbaumer, L., and Blackshear, P. J. (2008) *J. Biol. Chem.* **283,** 2586–2594
49. Vlasova, I. A., Tahoe, N. M., Fan, D., Larsson, O., Rattenbacher, B., Sternjohn, J. R., Vasdewani, J., Karypis, G., Reilly, C. S., Bitterman, P. B., and Bohjanen, P. R. (2008) *Mol. Cell* **29,** 263–270
50. Mayho, M., Fenn, K., Craddy, P., Crosthwaite, S., and Matthews, K. (2006) *Nucleic Acids Res.* **34,** 5312–5324
51. Tielens, A. G., and van Hellemond, J. J. (2009) *Trends Parasitol.* **25,** 482–490
52. Guo, X., Ma, J., Sun, J., and Gao, G. (2007) *Proc. Natl. Acad. Sci. U.S.A.* **104,** 151–156
53. Montagna, G. N., Donelson, J. E., and Frasch, A. C. (2006) *J. Biol. Chem.* **281,** 33949–33958
54. Silva, M. S., Prazeres, D. M., Lança, A., Atouguia, J., and Monteiro, G. A. (2009) *Parasitol. Res.* **105,** 1223–1229
55. Rotureau, B., Gego, A., and Carme, B. (2005) *Exp. Parasitol.* **111**, 207–209